Hindawi Publishing Corporation
Mathematical Problems in Engineering
Volume 2016, Article ID 4396296, 6 pages
http://dx.doi.org/10.1155/2016/4396296

Research Article

Elastic-Plastic Endochronic Constitutive Model of 0Crl7Ni4Cu4Nb Stainless Steels

Jinquan Guo,[1] Lianping Wu,[1] Xiaoxiang Yang,[1] and Shuncong Zhong[1,2]

[1]*School of Mechanical Engineering and Automation, Fuzhou University, Fuzhou 350108, China*
[2]*Department of Naval Architecture, Ocean and Marine Engineering, University of Strathclyde, Glasgow G4 0LZ, UK*

Correspondence should be addressed to Shuncong Zhong; zhongshuncong@hotmail.com

Received 13 August 2015; Accepted 17 January 2016

Academic Editor: Fabio De Angelis

We presented an elastic-plastic endochronic constitutive model of 0Crl7Ni4Cu4Nb stainless steel based on the plastic endochronic theory (which does not need the yield surface) and experimental stress-strain curves. The key feature of the model is that it can precisely describe the relation of stress and strain under various loading histories, including uniaxial tension, cyclic loading-unloading, cyclic asymmetric-stress axial tension and compression, and cyclic asymmetric-stress axial tension and compression. The effects of both mean stress and amplitude of stress on hysteresis loop based on the elastic-plastic endochronic constitutive model were investigated. Compared with the experimental and calculated results, it is demonstrated that there was a good agreement between the model and the experiments. Therefore, the elastic-plastic endochronic constitutive model provides a method for the accurate prediction of mechanical behaviors of 0Crl7Ni4Cu4Nb stainless steel subjected to various loadings.

1. Introduction

Due to the advantages of good corrosion resistance, formability, and mechanical behaviors, 0Crl7Ni4Cu4Nb stainless steel has been widely used in the automotive, aerospace engineering, and other industries [1, 2]. It is also an ideal material for self-lubricating bearings in aerospace industry. Parts made of 0Crl7Ni4Cu4Nb stainless steel usually can be mostly obtained at room temperature by plastic processing which generally involves the behaviors of material nonlinearity, geometric nonlinearity, and contact nonlinearity. Therefore, in order to improve the product quality, deformation behavior, damage mechanism, and structural response of 0Crl7Ni4Cu4Nb stainless steel are needed to be investigated. Finite element method is one of the methods to simulate the plastic forming process. Establishing a simple and practical constitutive model is the key issue for the research.

For the research of forming process, except the famous classic constitutive model [3, 4], many scholars have proposed some constitutive models for real engineering applications. Prager [5] and Ziegler [6] proposed the simple movement strengthen plastic models and J2 flow models based on von Mises yield surface. These constitutive models are based on the existence of yield surface and they are mainly related to the initial yield criterion, hardening rules, flow rule, and loading-unloading criterion. Computational issues and numerical applications were illustrated by De Angelis [7] for describing the mechanical behavior of rate-dependent plasticity models. Bergström and Boyce [8] probed the material response of carbon-black-filled chloroprene rubber subjected to different time-dependent strain histories using experimental method. De Angelis and Taylor [9, 10] adopted numerical algorithms for the computational modeling of plasticity problems with nonlinear kinematic hardening rules and presented a comparative analysis of linear and nonlinear kinematic hardening rules in computational elastoplasticity. However, the traditional constitutive model may affect the accuracy of plastic forming model since there is no obvious yield surface for 0Crl7Ni4Cu4Nb stainless steel. In order to solve the problem of traditional constitutive theories, Valanis [11] proposed the concept of viscoplastic theory without using yield surfaces. He used internal variables to characterize the material behavior and deformation law and finally established a plastic constitutive model which is similar to viscoelastic constitutive

model. The proposed model described elastic-plastic material behavior during unloading process. He also proposed analytical methods for engineering applications. Subsequently, Peng and Fan [12] developed a numerical analysis method on nonclassical plasticity theory based on pioneered Valanis constitutive theory. The developed theory improved the accuracy and convergence of Valanis's algorithm. Jain [13] established numerical integration methods leading to solutions of boundary value problems by the endochronic theory. Zeng et al. [14] proposed an endochronic numerical manifold method algorithm for elastoplasticity analysis. Bykov and Martynova [15] developed a method for determining the material functions of nonlinear endochronic theory of aging viscoelastic materials with preliminary mechanical damage.

In the present work, taking the concept of Valanis constitutive model without using the yield surface, an elastic-plastic endochronic constitutive model of 0Crl7Ni4Cu4Nb stainless steel was established based on irreversible thermodynamics of internal variables and using the endochronic theory and true stress-train curves of 0Crl7Ni4Cu4Nb stainless steel. Based on the endochronic constitutive model, mechanical behaviors of 0Crl7Ni4Cu4Nb stainless steel under the conditions of cyclic loading-unloading and cyclic tension and compression are analyzed. The effects of both mean stress and amplitude of stress on hysteresis loop based on the elastic-plastic endochronic constitutive model were investigated by experiments and computations. Compared with the experimental and calculated results, it is demonstrated that there was a good agreement between the model and the experiments. The results provide a theoretical basis for making plastic molding process of 0Crl7Ni4Cu4Nb stainless steel.

2. Experimental Materials and Methods

Experimental materials are 0Crl7Ni4Cu4Nb stainless steels with the following mass percent composition: C 0.04%–0.07%, Si 0.3%–1%, Mn 0.7%–1%, P 0.02%–0.04%, S 0.01%–0.03%, Cr 15%–17.5%, Ni 3%–5%, Nb 0.35%–0.45%, Cu 3%–5%, Mo 0.3%–0.5%, and Fe the remains. The specimens made of 0Crl7Ni4Cu4Nb stainless steel were Ø10 mm polished cylinders with a length of 30 mm.

Tensile tests and cyclic tension and compression tests were conducted by universal testing machine CMT5105 (SANS-MTS, China) with 1 mm/min strain rate at room temperature. In order to study the influence of mean stress and amplitude of stress on the stress-strain hysteresis loop, asymmetric axial stress cycle tests were conducted under the following two conditions. (a) Stress amplitude (σ_a) was 1700 Mpa and the average stress (σ_m) was 0 Mpa, 30 Mpa, and 60 Mpa; (b) the average stress was 60 Mpa and stress amplitudes were 1580 MPa, 1640 Mpa, and 1700 Mpa. Figure 1 showed the axial stress profile of the cyclic loading path where σ_a is equal to half of $\Delta\sigma$. During the test, the strain of the specimen was measured by an extensometer. Each test was conducted at least three times to eliminate the effect of the random factors in the experiment and the mean value of the test results was adopted.

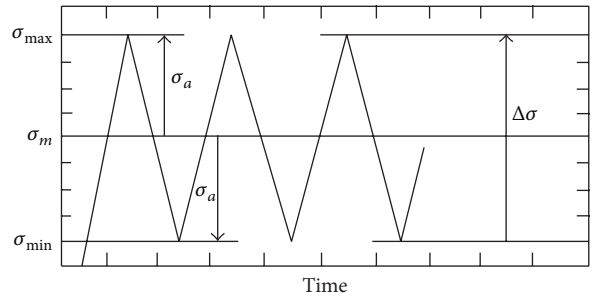

Figure 1: Axial stress profile of the cyclic loading.

3. Elastic-Plastic Endochronic Constitutive Model and Its Solution

3.1. Elastic-Plastic Endochronic Constitutive Model. It was assumed that the materials were initially isotropic and unrelated to plastic incompressible rate. Based on irreversible thermodynamics of internal variables, the endochronic constitutive relation is defined as [16]

$$\sigma_{ij} = \frac{E\nu}{(1+\nu)(1-2\nu)}\varepsilon^e_{kk}\delta_{ij} + 2G\varepsilon^e_{ij}, \tag{1}$$

$$s_{ij} = 2\int_0^z \rho\left(z - z'\right)\frac{\mathrm{d}\varepsilon^p_{ij}\left(z'\right)}{\mathrm{d}z}\mathrm{d}z', \tag{2}$$

$$s_{ij} = \sigma_{ij} - \frac{1}{3}\sigma_{kk}\delta_{ij}, \tag{3}$$

$$\varepsilon_{ij} = \varepsilon^e_{ij} + \varepsilon^p_{ij}, \tag{4}$$

$$\mathrm{d}z = \frac{\mathrm{d}\zeta}{f(\zeta)}, \tag{5}$$

$$\mathrm{d}\zeta = \left(\mathrm{d}\varepsilon^p_{ij}\mathrm{d}\varepsilon^p_{ij}\right)^{1/2}, \tag{6}$$

where $\rho(z)$ is kernel function, $f(\zeta)$ is hardening function, σ_{ij} is true stress tensor, s_{ij} is true partial stress tensor, ε_{ij} is true strain tensor, superscripts e and p mean elastic and plastic parts, ζ is plastic strain arc that represent historical effect in constitutive equation, $\mathrm{d}\zeta$ is distance between two plastic strain states, and z is a variable to characterize time in the endochronic constitutive equation.

The kernel function can be expressed in Dirichlet Series form [17]:

$$\rho(z) = \sum_{r=1}^{m} C_r e^{-a_r z}, \tag{7}$$

where m is the order of Dirichlet Series, C_1 is greater than or equal to 0, a_1 is equal to 0, and C_r and a_r are both positive when $r \geq 2$ and satisfy the following relations:

$$\sum_{r=2}^{m} C_r = \infty,$$
$$\sum_{r=2}^{m} \frac{C_r}{a_r} < \infty. \tag{8}$$

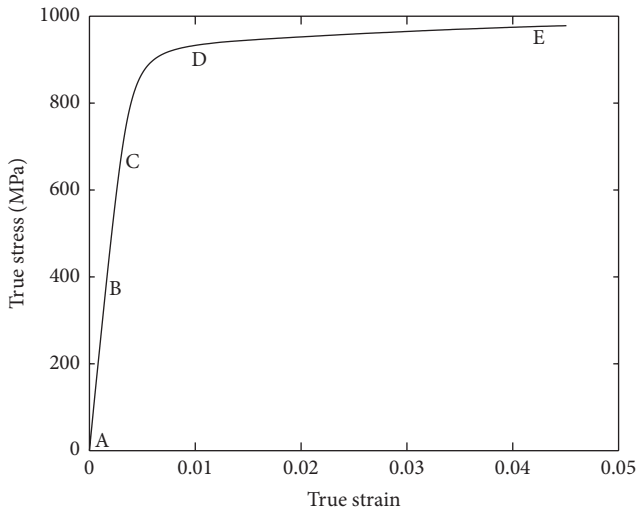

Figure 2: True stress-strain curve of 0Crl7Ni4Cu4Nb stainless steel.

For hardening function, it satisfies the following differential equation [18]:

$$\frac{\mathrm{d}f(z)}{\mathrm{d}z} = \beta\left(d - f(z)\right), \quad f(0) = 1, \tag{9}$$

where β is a parameter associated with the hardening rate and d is the plastic strain amplitude associated with loading path.

3.2. Analysis of True Stress-Strain Curve. Figure 2 shows true stress-strain curve of 0Crl7Ni4Cu4Nb obtained at room temperature under quasistatic condition. As shown in the figure, the material has no apparent yield point. During the early deformation, the material is at elastic stage where there is a linear relationship between stress and strain and the stress increases rapidly with strain increase. As the deformation increases, the material plastic deformation begins and the stress curve gradually becomes smooth with strain increase.

3.3. Solution of Kernel Function. According to [19], let $m = 4$, $C_1 = 0$, and $a_1 = 0$, and (7) can be expressed as

$$\rho(z) = C_2 e^{-a_2 z} + C_3 e^{-a_3 z} + C_4 e^{-a_4 z}. \tag{10}$$

Elastic modulus can be measured by one-directional tensile test and the result is $E = 196000$ MPa. According to the methods in [16], $C_4 e^{-a_4 z}$ can simulate the linear segment AB as shown in Figure 2 whilst $C_3 e^{-a_3 z}$ and $C_2 e^{-a_2 z}$ can simulate separately segment BC and segment CD. These six material parameters are calculated by numerical methods in the paper.

On the basis of endochronic constitutive theory, substituting (1) into (2), one can get the following equation:

$$s_{ij} = \sum_{r=1}^{n}\left[2\int_0^z C_r e^{-a_r(z-z')}\frac{\mathrm{d}\varepsilon_{ij}^p\left(z'\right)}{\mathrm{d}z'}\mathrm{d}z'\right]. \tag{11}$$

According to Hsu's method [16], the load can be divided into m steps. One can get

$$\left(s_{ij}\right)_m \approx \sum_{r=1}^{n}\left(s_{ij}^r\right)_m, \tag{12}$$

where $(s_{ij}^r)_m = (s_{ij}^r)_{m-1}e^{-a_r\Delta z_m} + 2(C_r/a_r)((\Delta\varepsilon_{ij}^p)_m/\Delta z_m)(1 - e^{-a_r\Delta z_m})$.

Constitutive equations in incremental form can be obtained by (11) and (12) as

$$\left(\Delta s_{ij}\right)_m = 2\left[\frac{f}{\Delta z_m}\sum_{r=1}^{n}\frac{C_r}{a_r}\left(1 - e^{-a_r\Delta z_m/f}\right)\right]\left(\Delta\varepsilon_{ij}^p\right)_m + \sum_{r=1}^{n}\left(s_{ij}^r\right)_{m-1}\left(e^{-a_r\Delta z_m/f} - 1\right), \tag{13}$$

where $(\Delta s_{ij})_m = (\Delta\sigma_{ij})_m - (1/3)(\Delta\sigma_{kk})_m\delta_{ij}$.

From (9), hardening function $f \approx 1$ when plastic deformation is small during initial deformation. So we can assume that hardening function equals 1 ($f = 1$). Therefore, the incremental constitutive equation of one-directional tensile can be derived by combining (13) and (6):

$$\left(\Delta\sigma_{11}\right)_m = 3\left[\frac{1}{\Delta\zeta_m}\sum_{r=1}^{n}\frac{C_r}{a_r}\left(1 - e^{-a_r\Delta\zeta_m}\right)\right]\left(\Delta\varepsilon_{11}^p\right)_m + \frac{3}{2}\sum_{r=1}^{n}\left(s_{11}^r\right)_{m-1}\left(e^{-a_r\Delta\zeta_m} - 1\right). \tag{14}$$

Substituting the previous obtained material parameters into (14), we can calculate the true stress-strain value. After comparing stress-strain curves predicted by model with those measured in tensile test and adjusting material parameters using trial-and-error method, we get the kernel function as

$$\rho(z) = 23500e^{-450z} + 200000e^{-2000z} + 11900000e^{-51900z}. \tag{15}$$

3.4. Solution of Hardening Function. Hardening function mainly describes the changes of line segment DE, as shown in Figure 2. According to [20], d was assumed to be constant, so hardening function can be derived from (9) as the following:

$$f(z) = d - (d-1)e^{-\beta z}, \tag{16}$$

where d and β are both material parameters to be determined.

Substituting (16) into (13), we can get the following equation:

$$\left(\Delta\sigma_{11}\right)_m = 3\left[\frac{d - (d-1)e^{-\beta z}}{\Delta\zeta_m}\sum_{r=1}^{n}\frac{C_r}{a_r} \cdot \left(1 - e^{-a_r\Delta\zeta_m/(d-(d-1)e^{-\beta z})}\right)\right]\left(\Delta\varepsilon_{11}^p\right)_m + \frac{3}{2} \cdot \sum_{r=1}^{n}\left(s_{11}^r\right)_{m-1}\left(e^{-a_r\Delta\zeta_m/(d-(d-1)e^{-\beta z})} - 1\right). \tag{17}$$

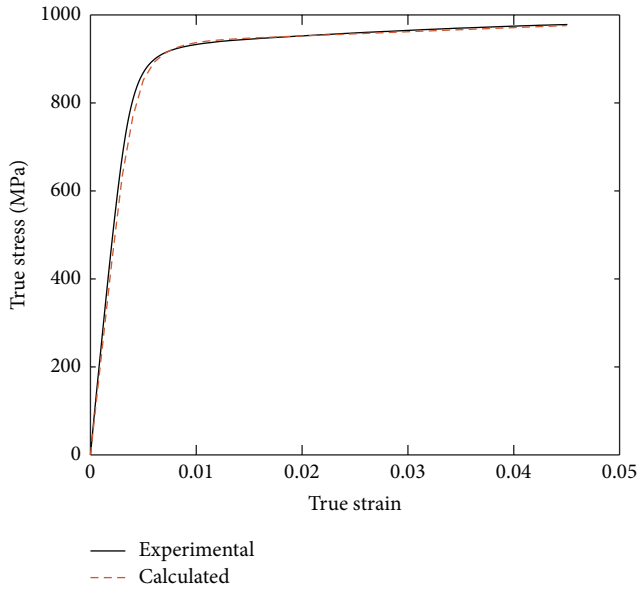

Figure 3: True stress-strain curves predicted by the elastic-plastic endochronic constitutive model and measured under quasistatic condition.

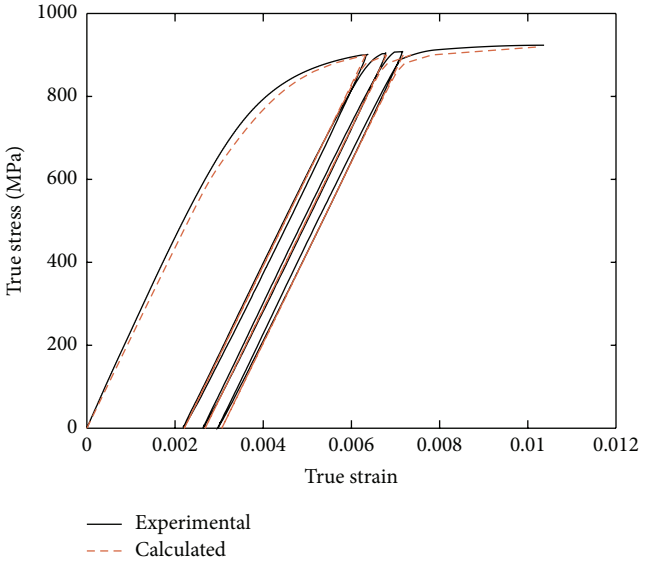

Figure 4: Comparison between experimental and simulated stress-strain curves for the loading-unloading tests of 0Crl7Ni4Cu4Nb stainless steel.

Substituting parameters related to kernel function into (17) and fitting the line segment DE in true stress-strain curve by using least square method, we can get $\beta = 1$ and $d = 1.85$. Subsequently, expression of hardening function can be obtained as

$$f(z) = 1.85 - 0.85e^{-z}. \tag{18}$$

Finally, substituting expressions of kernel function and hardening function into constitutive equations (1) to (6), the elastic-plastic endochronic constitutive model of 0Crl7Ni4Cu4Nb stainless steel at room temperature under quasistatic condition can be obtained.

4. Validations and Applications of the Constitutive Model

4.1. The Constitutive Model Validated by Experiments. Figure 3 showed the comparison of true stress-strain curves of 0Crl7Ni4Cu4Nb calculated by the elastic-plastic endochronic constitutive model and the experimental result. As can be seen from the figure, it demonstrated that there is a good agreement between the calculated and experimental true stress-strain curves.

Generally, springback and secondary yielding have significant influence on plastic forming process of parts, which may occur during unloading process and loading process with local unloading. Therefore, proper constitutive model should be able to describe response characteristics of materials during unloading and reloading process. In order to check whether the model can describe characteristics of unloading and reloading, loading-unloading tests of 0Crl7Ni4Cu4Nb were conducted. The comparison of calculated and experimental stress-strain curves is shown in Figure 4. It can be seen from the figure that the results calculated by the endochronic constitutive model are consistent well with the experimental ones.

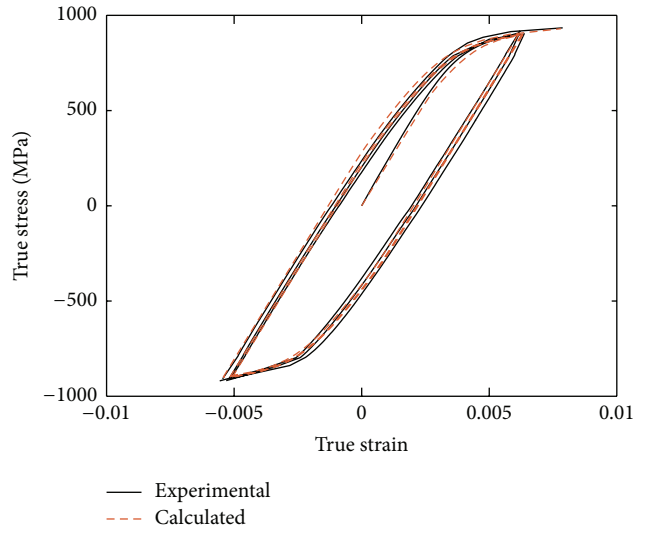

Figure 5: Comparison between experimental result and simulated stress-strain curves for the uniaxial unloading-reloading cycles tests of 0Crl7Ni4Cu4Nb stainless steel.

Comparison between experimental result and simulated stress-strain curves for the uniaxial unloading-reloading cyclic tests of 0Crl7Ni4Cu4Nb stainless steel is shown in Figure 5. It demonstrated that the endochronic constitutive model can accurately describe true stress-strain relationship under uniaxial unloading-reloading cycles.

4.2. Applications of the Constitutive Model. The mean stress and amplitude of stress on the hysteresis loop of parts can

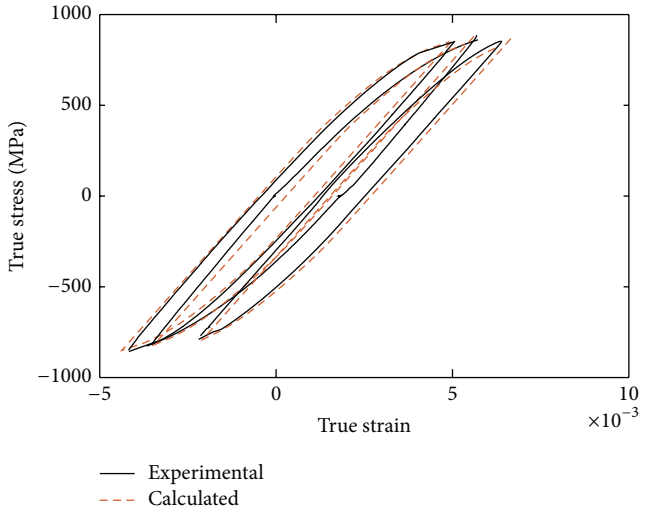

Figure 6: Comparison of experimental and simulated stress-strain curves for three different mean stresses of 0 MPa, 30 MPa, and 60 MPa with the stress amplitudes of 1700 MPa for 0Crl7Ni4Cu4Nb stainless steel.

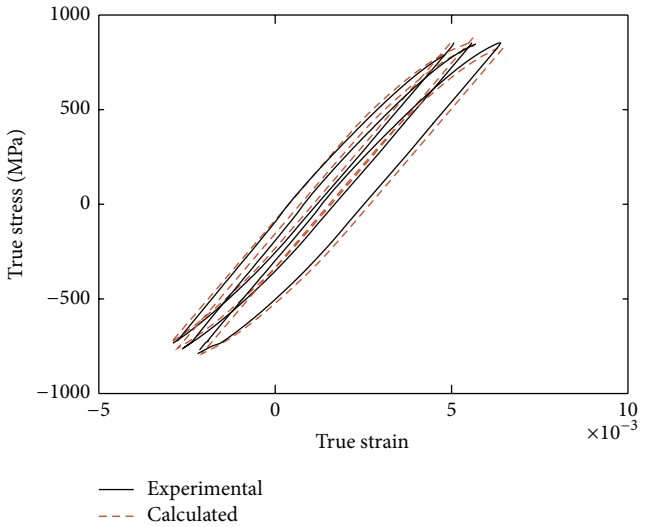

Figure 7: Comparison of experimental and simulated stress-strain curves for three different stress amplitudes of 1580 MPa, 1640 MPa, and 1700 MPa with the mean stress of 60 MPa for 0Crl7Ni4Cu4Nb stainless steel.

reflect deformation characteristics, stiffness degradation, and energy consumption under repeated uniaxial stress tests. The plastic deformation ability of parts can be determined by the shape of the hysteresis loop [21]. In order to study the mechanical properties of 0Crl7Ni4Cu4Nb stainless steel and the applications of the endochronic constitutive model, the influence of mean stress and amplitude of stress on the hysteresis loop were investigated in the present work. The hysteresis loop of parts can be obtained by loading asymmetric cycle stress. Figure 6 showed the comparison of experimental and simulated stress-strain curves for three different mean stresses as 0 MPa, 30 MPa, and 60 MPa with the stress amplitudes of 1700 MPa for 0Crl7Ni4Cu4Nb stainless steel. As can be seen from Figure 6, the results calculated by the model are consistent well with the experimental ones. Furthermore, the mean stress has little influence on hysteresis loop shape; also, hysteresis loop shifts up with increment of mean stress. Besides, the plump hysteresis loop reflects good plastic deformability of 0Crl7Ni4Cu4Nb stainless steel.

Comparison of experimental and simulated stress-strain curves for three different stress amplitudes of 1580 MPa, 1640 MPa, and 1700 MPa with the mean stress of 60 MPa for 0Crl7Ni4Cu4Nb stainless steel is shown in Figure 7. The figure shows there is a good agreement with the results calculated by the experimental and calculated results. Besides, hysteresis loop, plastic deformation, and energy consumption all increase with the increment of stress amplitude.

5. Conclusions

In summary, uniaxial tensile test, cyclic loading-unloading test, cyclic symmetry-stress axial tension-compression test, and cyclic asymmetric-stress axial tension-compression test for cylindrical parts made of 0Crl7Ni4Cu4Nb stainless steel were conducted by universal testing machine CMT5105 at room temperature under quasistatic conditions. The corresponding true stress-strain curves and true stress-strain hysteresis loops are obtained. On the basis of the plastic endochronic theory and uniaxial tension stress-strain curves of 0Crl7Ni4Cu4Nb stainless steel, the elastic-plastic endochronic constitutive model of 0Crl7Ni4Cu4Nb stainless steel was built on by using the endochronic theory without the yield surface.

True stress-strain hysteresis loops of uniaxial tensile test, loading-unloading test, cyclic axial symmetry stress and tension test, and asymmetric axial tension-compression stress test were calculated by using the endochronic constitutive model. The effects of both mean stress and amplitude of stress on hysteresis loop based on the elastic-plastic endochronic constitutive model were investigated by experiments and computations. Compared with the experimental and calculated results, it is demonstrated that there was a good agreement between the model and the experiments. Therefore, the elastic-plastic endochronic constitutive model could be a theoretical basis to simulate plastic molding process of the material and could provide a method for the accurate prediction of mechanical behaviors of 0Crl7Ni4Cu4Nb stainless steel subjected to various loadings. The constitutive model could be employed to mimic the extruded forming process of stainless steel, and unloading and reloading process of stainless steel. This will be considered as future work.

Conflict of Interests

The authors declare that there is no conflict of interests regarding the publication of this paper.

Acknowledgments

The authors gratefully acknowledge support from Fujian Provincial Science and Technology Major Project (2012HZ0006-3), the National Natural Science Foundation of China (11372074, 51005077), the Fujian Provincial Excellent Young Scientist Fund (2014J07007), the Specialised Research Fund for the Doctoral Program of Higher Education, the Ministry of Education, China (20133514110008), the Ministry of Health, China (WKJ-FJ-27), Fujian Provincial Natural Science Foundation (2015J01234), and Fujian Provincial Quality and Technical Supervision Bureau Project (FJQI2014008, FJQI2013024).

References

[1] C. R. Das, H. C. Dey, G. Srinivasan, S. K. Albert, A. K. Bhaduri, and A. Dasgupta, "Weldability of 17-4PH stainless steel in overaged heat treated condition," *Science and Technology of Welding and Joining*, vol. 11, no. 5, pp. 502–508, 2006.

[2] M. R. Tavakoli Shoushtari, M. H. Moayed, and A. Davoodi, "Post-weld heat treatment influence on galvanic corrosion of GTAW of 17-4PH stainless steel in 3.5% NaCl," *Corrosion Engineering Science and Technology*, vol. 46, no. 4, pp. 415–424, 2011.

[3] J. Oliver, "Modelling strong discontinuities in solid mechanics via strain softening constitutive equations. Part 1: fundamentals," *International Journal for Numerical Methods in Engineering*, vol. 39, no. 21, pp. 3575–3600, 1996.

[4] K. Huang and Y. Huang, *The Constitutive of Solid*, Tsinghua University Press, Beijing, China, 1999.

[5] W. Prager, "A new method of method of analyzing stress and strain in work-hardening plastic solid," *Journal of Applied Mechanics*, vol. 7, pp. 493–496, 1956.

[6] H. Ziegler, "A modification of Prager's hardening rule," *Quarterly of Applied Mathematics*, vol. 17, pp. 55–65, 1959.

[7] F. De Angelis, "Computational issues and numerical applications in rate-dependent plasticity," *Advanced Science Letters*, vol. 19, no. 8, pp. 2359–2362, 2013.

[8] J. S. Bergström and M. C. Boyce, "Constitutive modeling of the large strain time-dependent behavior of elastomers," *Journal of the Mechanics and Physics of Solids*, vol. 46, no. 5, pp. 931–954, 1998.

[9] F. De Angelis and R. Taylor, "Numerical algorithms for plasticity models with nonlinear kinematic hardening," in *Proceedings of the 11th World Congress on Computational Mechanics (WCCM '14)*, Barcelona, Spain, July 2014.

[10] F. de Angelis, "A comparative analysis of linear and nonlinear kinematic hardening rules in computational elastoplasticity," *Technische Mechanik*, vol. 32, no. 2, pp. 164–173, 2012.

[11] K. Valanis, "Fundamental consequences of a new intrinsic time measure: plasticity as a limit of the endochronic theory," Document 1-65, DTIC (Division of Materials Engineering, The University of Iowa), Iowa City, Iowa, USA, 1978.

[12] X. Peng and J. Fan, "A numerical approach for nonclassical plasticity," *Computers & Structures*, vol. 47, no. 2, pp. 313–320, 1993.

[13] S. K. Jain, "Material modeling by endochronic theory: the Virginia tech experience," *International Journal for Computational Methods in Engineering Science and Mechanics*, vol. 13, no. 5, pp. 329–333, 2012.

[14] W. Zeng, J. Li, and F. Kang, "Numerical manifold method with endochronic theory for elastoplasticity analysis," *Mathematical Problems in Engineering*, vol. 2014, Article ID 592870, 11 pages, 2014.

[15] D. L. Bykov and E. D. Martynova, "Numerical-graphical method for determining characteristics of damaged viscoelastic materials," *Mechanics of Solids*, vol. 48, no. 4, pp. 410–416, 2013.

[16] S. Y. Hsu, S. K. Jain, and O. H. Griffin Jr., "Verification of endochronic theory for nonproportional loading paths," *Journal of Engineering Mechanics*, vol. 117, no. 1, pp. 110–131, 1991.

[17] H. C. Wu and R. J. Yang, "Application of the improved endochronic theory of plasticity to loading with multi-axial strain-path," *International Journal of Non-Linear Mechanics*, vol. 18, no. 5, pp. 395–408, 1983.

[18] J. Fan and X. Peng, "A physically based constitutive description for non-proportional cyclic plasticity," *Journal of Engineering Materials and Technology*, vol. 113, pp. 254–262, 1991.

[19] X. Peng, Y. Qin, and R. Balendra, "FE analysis of springback and secondary yielding effect during forward extrusion," *Journal of Materials Processing Technology*, vol. 135, no. 2-3, pp. 211–218, 2003.

[20] X. Peng and A. R. S. Ponter, "A constitutive law for a class of two-phase materials with experimental verification," *International Journal of Solids and Structures*, vol. 31, no. 8, pp. 1099–1111, 1994.

[21] Y.-M. Jen and Y.-C. Chiou, "Application of the endochronic theory of plasticity for life prediction with asymmetric axial cyclic straining of AISI 304 stainless steel," *International Journal of Fatigue*, vol. 32, no. 4, pp. 754–761, 2010.